AAEC/TM371

AUSTRALIAN ATOMIC ENERGY COMMISSION

RESEARCH ESTABLISHMENT

LUCAS HEIGHTS

TEMPERATURES AND THERMO-ELASTIC STRESS IN SPHERICALLY SYMMETRIC FUEL ELEMENTS WITH VARYING MATERIAL PROPERTIES

by

IAN M. BINNS

February 1967

AUSTRALIAN ATOMIC ENERGY COMMISSION

RESEARCH ESTABLISHMENT

LUCAS HEIGHTS

TEMPERATURES AND THERMO-ELASTIC STRESS IN SPHERICALLY SYMMETRIC FUEL ELEMENTS WITH VARYING MATERIAL PROPERTIES

by

IAN M. BINNS

ABSTRACT

In the thermo-elastic stress analysis of a spherically symmetric fuel element as used in a pebble bed reactor the problems of a radial variation in material properties and the temperature dependence of these properties can be unified into a single analysis. Such an analysis is developed for incorporation in a computer programme and applied, as an example, to a fuel element for a beryllia moderated reactor. The results give the effect of different material properties between surface and centre, a buffer layer between surface coating and centre, an increase in temperature of a fuel element composed of materials with different properties, and temperature dependence of the fuel element materials.

CONTENTS

1. INTRODUCTION

The thermo-elastic stress analysis of a spherical fuel element as used in a pebble bed reactor is usually based on spherical symmetry assuming homogeneous material with constant properties throughout the fuel element. Where there is variation in material properties which affect the temperature distribution only, and the temperature distribution can be determined in an analytic form, then the stress distribution can be simply determined. This is the case for concentric shells with different thermal conductivities and heat production (Binns 1964). The effect of variation in property values including elastic properties, whether spatial or temperature dependent, is more difficult as it requires continuity of temperature, displacement, and stress, the latter across the plane of action only. The problem can be simplified if mean values of the properties are assumed, however, the choice of values is difficult depending on the accuracy required in the calculations.

Baltrukonis (1959), studying a thick-wall cylinder, concluded that there is no preferred method over the complex numerical approach, particularly in the range of high temperatures where properties vary rapidly. However, it is recognised that in this range the assumption of elastic behaviour is not well founded. (Morozov and Fridman 1962). An appreciation of the effect of the temperature dependence of the material properties is necessary even for the elastic assumption since the solutions can be regarded as the initial solutions for any subsequent stress relaxation if the loading takes place over a short time.

For the spherically symmetric fuel element the analysis involving temperature dependence can be made identical to that of a fuel element consisting of many different materials and the following analysis is general for the spherically symmetric case. It was undertaken as part of the A.A.E.C.'s pebble bed reactor study which considered fuel elements with a fission product retentive coating and other configurations where the fuel was distributed in various ways.

This report describes the method of analysis and gives typical results which indicate that stresses based on the assumption of a homogeneous fuel element may be significantly different to those accounting for the varying material properties.

2. FUEL ELEMENT MODEL

The model is a spherically symmetric fuel element composed of a series of N concentric shells. The n^{th} region or shell starting at the centre is contained within the bounds of radii r_{n-1} and r_n. Conditions are constant with respect to time and the material is isotropic with uniform properties in each region. Contact is maintained between adjacent shells at all times with no slip. Adjacent shells

may be of the same material but with different properties corresponding to the different mean temperatures.

3. TEMPERATURE DISTRIBUTION

For spherical symmetry the heat conduction equation for isotropic uniform material:

$$\nabla^2 T = -\frac{q}{k} \quad , \qquad \text{.....(1)}$$

leads to the temperature equation for the n^{th} shell:

$$T = A_n r^2 + B_n r^{-1} + C_n \quad . \qquad \text{.....(2)}$$

A_n, B_n, and C_n are constants determined for each shell as follows:

With perfect contact between each shell there is continuity of magnitude of temperature but not necessarily of spatial differential coefficient of the temperature. In the steady state, from the thermal balance at the boundaries of the n^{th} shell:

$$-K_n \left(\frac{dT}{dr}\right)_n = \frac{1}{r_n^2} \sum_{i=1}^{n} \frac{r_i^3 - r_{i-1}^3}{3} q_i \quad \text{at } r = r_n \quad , \qquad \text{.....(3)}$$

$$-K_n \left(\frac{dT}{dr}\right)_n = \frac{1}{r_{n-1}^2} \sum_{i=1}^{n-1} \frac{r_i^3 - r_{i-1}^3}{3} q_i \quad \text{at } r = r_{n-1} \quad . \qquad \text{.....(4)}$$

Writing $\Sigma_n = \sum_{i=1}^{n} \frac{r_i^3 - r_{i-1}^3}{3} q_i$ and defining Σ_o as zero

and r_o as zero or finite, then by substituting Equation 2 in (3) and (4) the following are obtained:

$$A_n = - \frac{q_n}{6 K_n} \qquad \text{.....(5)}$$

$$B_n = - \frac{r_{n-1}^3 \Sigma_n - r_n^3 \Sigma_{n-1}}{K_n (r_n^3 - r_{n-1}^3)} \quad . \qquad \text{.....(6a)}$$

If zero magnitude is assigned to a hypothetical q_o then:

$$B_n = - \frac{1}{3K_n} \sum_{i=o}^{n-1} r_i^3 (q_{i+1} - q_i) \quad . \qquad \text{.....(6b)}$$

By equating temperatures at the interface and assigning T_s as the fuel element surface temperature the remaining constant C_n is given by:

$$C_n = \sum_{i=n}^{N-1} \left(A_{i+1} r_i^2 + B_{i+1} r_i^{-1} \right) - \sum_{i=n}^{N} \left(A_i r_i^2 + B_i r_i^{-1} \right) + T_s \quad ,$$

and for the N^{th} and outermost shell:

$$C_N = -A_N r_N^2 - B_N r_N^{-1} + T_s \quad . \qquad \text{.....(7)}$$

4. STRESS DISTRIBUTION

For an elastic system in spherical symmetry, the thermal stresses and radial displacement can be obtained (Timoshenko and Goodier 1951) from the following equations:

$$\sigma_r = -\left(\frac{2 E \alpha}{1 - \nu}\right)_n \frac{1}{r^3} \int_{r_{n-1}}^{r} Tr^2 \, dr + \left(\frac{E D}{1 - 2\nu}\right)_n - \left(\frac{2 E G}{1 + \nu}\right)_n \frac{1}{r^3} \quad , \qquad \text{.....(8)}$$

$$\sigma_t = \left(\frac{E \alpha}{1-\nu}\right)_n \left[\frac{1}{r^3} \int_{r_{n-1}}^{r} Tr^2 \, dr - T \right] + \left(\frac{E D}{1-2\nu}\right)_n + \left(\frac{E G}{1+\nu}\right)_n \frac{1}{r^3} \quad , \qquad \text{.....(9)}$$

$$u = \left(\frac{1 + \nu}{1-\nu} \alpha\right)_n \frac{1}{r^2} \int_{r_{n-1}}^{r} Tr^2 \, dr + Dr + G_n r^{-2} \quad , \qquad \text{.....(10)}$$

where r is within the n^{th} shell and the constants D and G are determined by the following boundary conditions:

1. At the centre, for a solid sphere the displacement is zero while for a hollow sphere the radial stress is zero at the inner boundary.
2. At the interfaces, both the radial stresses and displacements are continuous.
3. At the outer boundary, which is assumed free, the radial stress is zero.

It should be noted that the coefficient of thermal expansion used is the mean expansion per degree from some datum temperature at which no stress exists.

By substituting the temperature equation in the stress and displacement equation and then writing:

$$a_n = -\left(\frac{2E\alpha}{1-\nu}\right)_n \int_{r_{n-1}}^{r_n} Tr^2\,dr \quad ,$$

$$= -\left(\frac{2E\alpha}{1-\nu}\right)_n \left[A_n \frac{r_n^5 - r_{n-1}^5}{5} + B_n \frac{r_n^2 - r_{n-1}^2}{2} + C_n \frac{r_n^3 - r_{n-1}^3}{3} \right], \quad \ldots\ldots(11$$

$$b_n = \left(\frac{E}{1-2\nu_n}\right) \quad , \qquad \ldots\ldots(12$$

$$e_n = -\left(\frac{2E}{1+\nu}\right)_n \quad , \qquad \ldots\ldots(13$$

$$d_n = \left(\frac{1+\nu}{1-\nu}\alpha\right)_n \int_{r_{n-1}}^{r_n} Tr^2\,dr \quad , \qquad \ldots\ldots(14$$

$$= \left(\frac{1+\nu}{1-\nu}\alpha\right)_n \left[\frac{A_n}{5}\left(r_n^5 - r_{n-1}^5\right) + \frac{B_n}{2}\left(r_n^2 - r_{n-1}^2\right) + \frac{C_n}{3}\left(r_n^3 - r_{n-1}^3\right)\right],$$

the boundary conditions at the interfaces can be written for radial stress:

$$b_n D_n + \frac{e_n G_n}{r_{n-1}^3} = \frac{a_{n-1}}{r_{n-1}^3} + b_{n-1} D_{n-1} + \frac{e_{n-1} G_{n-1}}{r_{n-1}^3} \quad , \qquad \ldots\ldots(15)$$

and for displacement:

$$D_n r_{n-1} + G_n r_{n-1}^{-2} = d_{n-1} r_{n-1}^{-2} + D_{n-1} r_{n-1} + G_{n-1} r_{n-1}^{-2} \; . \qquad \ldots\ldots(16)$$

The boundary condition at the centre for a solid sphere, displacement zero, implies that $G_1 = 0$ from Equation 10. To satisfy the hollow sphere inner boundary condition that the radial stress be equal to zero, Equation 15 is used, defining:

$$a_o = b_o = e_o = 0 \quad .$$

To satisfy the outer boundary condition, that the radial stress be zero,

Equation 15 is used, defining:

$$a_{N+1} = b_{N+1} = e_{N+1} = 0 \quad .$$

Thus there are two equations for each interface and one each for the outer and inner fuel element boundary, the latter depending on whether it is a solid or hollow sphere.

By setting the elastic constants and expansion equal to zero the effect of a small gas gap can be analysed neglecting radiation effects which are assumed to be small with small difference in temperatures.

The following matrix equation is then solved to give the stress equation constants D_n and G_n, $n = 1, N$:

$$\begin{bmatrix}
b_1 r_o^3 & e_1 & & & & & & & & \\
0 & 1 & & & & & & & & \\
-b_1 r_1^3 & -e_1 & b_2 r_1^3 & e_2 & & & & & & \\
-r_1^3 & -1 & r_1^3 & 1 & & & & & & \\
 & & -b_2 r_2^3 & -e_2 & b_2 r_2^3 & e_3 & & & & \\
 & & -r_2^3 & -1 & r_2^3 & 1 & & & & \\
 & & & & -b_n r_n^3 & -e_n & b_{n+1} r_n^3 & e_{n+1} & & \\
 & & & & -r_n^3 & -1 & r_n^3 & 1 & & \\
 & & & & & & -b_{N-1} r_{N-1}^3 & -e_{N-1} & b_N r_{N-1}^3 & e_N \\
 & & & & & & -r_{N-1}^3 & -1 & r_{N-1}^3 & 1 \\
 & & & & & & & & -b_N r_N^3 & -e_N
\end{bmatrix}
\begin{Bmatrix} D_1 \\ G_1 \\ D_2 \\ G_2 \\ D_3 \\ G_n \\ D_{n+1} \\ G_{N-1} \\ D_N \\ G_N \end{Bmatrix}
=
\begin{Bmatrix} 0 \\ a_1 \\ d_1 \\ a_2 \\ d_2 \\ a_n \\ d_n \\ a_{N-1} \\ d_{N-1} \\ a_N \end{Bmatrix}$$

for hollow sphere / for solid sphere

$$\ldots\ldots(17)$$

Then the stresses are given by:

$$\sigma_r = -\left(\frac{2\,E\,\alpha}{1-\nu}\right)_n \frac{1}{r^3}\left[A_n \frac{r^5-r_{n-1}^5}{5} + B_n \frac{r^2-r_{n-1}^2}{2} + C_n \frac{r^3-r_{n-1}^3}{3}\right] + b_n D_n + e_n G_n r^{-3} \qquad .....(18)$$

$$\sigma_t = \left(\frac{E\,\alpha}{1-\nu}\right)_n \left\{\frac{1}{r^3}\left[A_n \frac{r^5-r_{n-1}^5}{5} + B_n \frac{r^2-r_{n-1}^2}{2} + C_n \frac{r^3-r_{n-1}^3}{3}\right] - T\right\} +$$

$$+ \; b_n D_n - \frac{1}{2} e_n G_n r^{-3} \qquad . \qquad .....(19)$$

The complexity of Equation 17 makes it impracticable to solve analytically beyond N = 2 and so use is made of a digital computer.

5. A NOTE ON THE COEFFICIENT OF THERMAL EXPANSION

The mean coefficient of thermal expansion is a function of the material, its temperature, and the datum temperature from which the expansion is measured, the latter usually being given as room temperature. Thermal stresses are produced by differential expansion due to change in temperature from some datum temperature where these stresses are zero. The thermal expansion used in the preceding analysis should therefore be based on this temperature at which stresses are zero.

The relation between coefficients based on different datum temperatures is derived as follows:

Let $\epsilon_{T_o,T}$ be the fractional expansion due to temperature increase T_o to T and $\alpha_{T_o,T}$ be the mean fractional expansion per degree temperature increase from T_o to T. T_z is the new datum temperature and ℓ is the length at T_o.

Therefore:

$$\epsilon_{T_o,T} = \alpha_{T_o,T}\,(T - T_o)$$

$$(1 + \epsilon_{T_z,T})\;(1 + \epsilon_{T_o,T_z})\,\ell = (1 + \epsilon_{T_o,T})\,\ell$$

$$\epsilon_{T_z,T} = \alpha_{T_z,T}\,(T - T_z) \qquad ,$$

and by substitution:

$$\alpha_{T_z,T} = \frac{\alpha_{T_o,T}\,(T-T_o) - \alpha_{T_o,T_z}}{(T-T_z)\,[1 + \alpha_{T_o,T_z}\,(T_z-T_o)]} \qquad , \qquad .....(20)$$

and in the limiting case:

$$\lim_{T \to T_z} \alpha_{T_z,T} = \frac{\alpha_{T_o,T_z} + (T_z-T_o)\left(\frac{d\alpha_{T_o,T}}{dT}\right)_{T=T_z}}{1 + \alpha_{T_o,T_z}\,(T_z - T_o)} \qquad . \qquad .....(21)$$

For example, when the fuel element is manufactured at a high temperature, on cooling to room temperature, residual stresses will exist if there is a spatial variation in material properties and it could be assumed that some temperature T_z exists such that there are no residual stresses. This temperature should therefore be the datum temperature of the coefficient of thermal expansion.

6. COMPUTER PROGRAMME

From input data of material properties, dimensions, and power density of each concentric region, the computer programme determines the temperature and thermoelastic stresses over a sphere for spherically symmetric conditions.

The material properties may be temperature dependent and an iterative procedure is used to determine the thermal conductivity and the resulting temperature distribution. Each region may be divided into a number of shells to account for this temperature dependence, and property values at the mean shell temperature are assigned to each shell.

Note that an analytic solution for a temperature dependent thermal conductivity is possible for the temperature distribution but when the conductivity is expressed as a series in temperature it would not lead to an easy solution in the analytic stress equations.

A flow chart of the program is given in Figure 8. The method used in solving Equation 17, is the Gauss-Jordon reduction method suggested by Ralston and Wilf (1959). This is incorporated into a sub-programme SID compiled by J. P. Pollard, (A.A.E.C., unpublished).

7. RESULTS AND DISCUSSION

The analysis is used to determine the thermo-elastic stress distributions of various spherical fuel elements with radially varying material properties. (Figure 9). The material properties used in the example are based on early data for beryllia and beryllia based dispersion fuel mixtures. More accurate data now available from Turner and Smith (1965) and Veevers and Rotsey (1966a, 1966b) should be used in any future calculation. For computation the information is converted to a polynomial equation in temperature using the Chebychoff polynomial curve-fitting programme of Hawker and Ridgway (1965). The resulting curves are shown in Figure 1.

As an example, a fuel element of $1\frac{1}{2}$ inch diameter is used. The mean fuel element power density is taken as 18.1818 watts/cm^3 which corresponds to 11 watts/cm^3 mean core power density for a randomly packed pebble bed. Zero stress is assumed to occur with a uniform temperature at 20°C.

7.1 Temperature Dependence of Material Properties

The effect of temperature dependence is shown in Figure 2, for a fuel surface temperature of 600°C on a fully homogeneous fuel element. The stress and temperatures are compared with those of a fuel element of uniform properties evaluated at the surface temperature. With uniform properties the stress distribution can be derived from the equation of Timoshenko and Goodier (1951) together with the general equation for temperature distribution giving:

$$\left.\begin{aligned} \sigma_r &= \frac{E\alpha_{inst}}{1-\mu} \quad \frac{b^2 q}{K} \left[\left(\frac{r}{b}\right)^2 - 1 \right] \frac{1}{15} \\ \sigma_t &= \frac{E\alpha_{inst}}{1-\mu} \quad \frac{b^2 q}{K} \left[2\left(\frac{r}{b}\right)^2 - 1 \right] \frac{1}{15} \end{aligned}\right\} \quad , \qquad .....(22)$$

where b is the fuel element radius.

The difference in the two sets of results is most noticeable at the centre where the assumption of uniform material properties leads to a stress 4 per cent. lower and a temperature 3 per cent. lower than the results for temperature dependent properties. At the surface the effect on stress is decreased to 2 per cent. difference. At higher temperatures the effect is found to be even smaller. Since the accuracy of material property values in general would contribute a much greater variation, the above difference can be neglected in the case of beryllia and the assumption of properties independent of temperature is fully

justified. Other materials with properties significantly different to beryllia would require an independent assessment.

7.2 Coated Fuel Element

The increase in stress due to the concentration of fuel in a centre core such that the ball is in effect coated with a layer of beryllia is indicated in Figure 3. The increase is affected by the difference in material properties between fuelled and unfuelled beryllia as well as a change in temperature distribution due to heat being produced only in the centre core. It is possible to isolate the effects of some of the material properties and of the change in temperature distribution.

It has been shown (Binns 1964) that the surface tangential stress in a sphere of radius r_2 with a heat producing centre core of radius r_1 and thermal conductivities K_1 and K_2 in the core and coating respectively, is given by:

$$\sigma_t = \sigma_1^* \left[\left(\frac{r_1}{r_2}\right)^2 + 2.5 \frac{K_1}{K_2} \left\{ 1 - \left(\frac{r_1}{r_2}\right)^2 \right\} \right] \quad , \qquad .....(23)$$

where σ_1^* is the stress of the equivalent homogeneous sphere with thermal conductivity K_1.

For uniform thermal conductivity this reduces to:

$$\sigma_t = \sigma^* \left[2.5 - 1.5 \left(\frac{r_1}{r_2}\right)^2 \right] \quad . \qquad .....(24)$$

The surface tangential stress due to different thermal expansion coefficients α_1 and α_2 in core and coating respectively can be shown to be:

$$\sigma_t = \sigma_1^* + \frac{E(\alpha_2 - \alpha_1)}{1-\nu} \left[\left\{ 1 - \left(\frac{r_1}{r_2}\right)^3 \right\} T_{\substack{coating \\ mean}} - T_{surface} \right] , \qquad .....(25)$$

where σ_1^* is the stress of the equivalent homogeneous sphere with thermal expansion coefficient α_1.

Similarly,

$$\sigma_t = \sigma_2^* + \frac{E(\alpha_1 - \alpha_2)}{1-\nu} \left(\frac{r_1}{r_2}\right)^3 T_{\substack{core \\ mean}} \quad , \qquad .....(26)$$

where σ_2^* is the stress of the equivalent homogeneous sphere with thermal expansion coefficient α_2.

Isolating the effect of elastic modulus requires an analysis based on the method used in this report, that is, matching the stresses and displacements at the interface.

From the above equations it can be seen that small differences in thermal conductivity of the coating and core of a spherical fuel element cause only small changes in stress compared with small differences in the thermal expansion coefficient. The latter difference is most important with thin coatings and its effect on stress is proportional to the operating temperature of the fuel element.

The effect of the difference in thermal expansion coefficient decreases as the coating thickness is increased. With the thicker coating, however, the change in stress (Equation 24) resulting from the new temperature distribution becomes more important. It has been suggested (D. R. Ebeling, A.A.E.E. private communication) that by purposely causing a difference in thermal expansion coefficient by the addition of impurities, the additional stress caused by the change temperature distribution could be significantly reduced.

7.3 Buffer Layer between Core and Coating

The effect of introducing a buffer region such as a layer of graphite, between the core and coating is shown in Figure 4. The material properties assumed for the graphite are:

Elastic modulus	0.8×10^{6} p.s.i.
Thermal expansion coefficient	0.65×10^{-6} degC^{-1}
Poisson's ratio	0.25
Thermal conductivity	0.523 watts cm^{-1} degC^{-1}

Consequently the graphite has an elastic modulus approximately 1/60th that of beryllia and a thermal expansion coefficient 2/3 that of beryllia. These differences allow the radial displacement of the centre core to be totally or partially absorbed in the region between core and coating thereby reducing the strain in the coating.

It is possible to optimise the buffer layer thickness assuming that it cannot support a radial tensile stress. The optimised geometry corresponds to zero radial stress existing at the inner boundary of the coating. The optimum buffer layer thickness and the corresponding surface tangential stress is shown in Figure 5. The gains through decreasing the stress are very significant when compared with the equivalent coated sphere. The effect would vary for different buffer material properties, with thinner layers required for lower elastic moduli.

A further advance on this concept is obtained when all heat is produced in the buffer layer itself. This then eliminates the high stresses in the core. The optimum buffer layer thickness is much reduced when the same material properties are assumed, since the displacement to be absorbed is much smaller. In practice the high concentration of fuel in the buffer region will change its properties but the concentration and thickness could be adjusted to give optimum stress.

A comparison of the above two buffer layer concepts is made with the equivalent coated ball in Figure 6, assuming the same coating thickness and power output.

7.4 Residual Stresses

As indicated by Equations 25 and 26 and in Section 5 there can be a significant portion of the stress which is dependent on the absolute temperature of the fuel element. At some temperature there will be a stress-free condition and if there is any difference in thermal expansion coefficient within the fuel element then at any other temperature, even if uniform, a thermal stress will exist.

The examples already given have assumed that zero stress occurs at a uniform temperature of 20°C. If in fact the zero stress free condition occurred at a uniform 1000°C it would be necessary to superimpose a residual stress at 20°C. The effect of two different datum temperatures for the coated fuel element is shown in Figure 7 based on the beryllia and standard fuel material properties mentioned above. The residual stress which is seen to be equal to the difference in the two resulting stresses is the stress existing at 20°C with no heat production.

7.5 Accuracy of the Matrix Inversion

Although the structure of the matrix in Equation 17 is such that negligible errors can be expected, an iterative procedure was used to check on the accuracy.

That is:

$$M_{n+1}^{-1} = M_{n}^{-1} \left[2I - MM_{n}^{-1} \right] ,$$

where M_{n}^{-1} is the n^{th} estimate of the inversion of the matrix M and I is the unit matrix.

No better accuracy was obtained with this method, using the inversion given by the programme discussed in this report as the first estimate.

8. CONCLUSIONS

The analysis developed was successfully incorporated into a computer programme making possible a study of radial varying material properties in a spherical fuel element.

With respect to the example of the beryllia based fuel element under study the following important results were obtained.

(i) Temperature dependence of material properties can be neglected for the uniformly heated homogeneous sphere.

(ii) Small decreases in the thermal expansion coefficients of the coating with respect to the centre core of the fuel element produce significantly higher stresses when compared with the equivalent homogeneous fuel element.

(iii) Stresses can be significantly reduced by incorporating a buffer interlayer between the fuel element core and coating. The buffer layer can be composed of material significantly lower in elastic modulus and/or thermal expansion than the material surrounding it.

The last two items are general conclusions in that they apply irrespective of the basic material property.

9. NOTATION

a, b, d, e	constants as defined in equations (11) to (14)
A, B, C	constants for temperature distribution equation (2).
D	constant for stress and displacement equations (8) to (10).
E	elastic modulus
G	constant for stress and displacement equations (8) to (10)
I	unit matrix
K	thermal conductivity

ℓ	length
M	matrix
n	number of shell commencing at centre of sphere
N	total number of shells
q	heat production per unit volume
r	radius
r_n	outer radius of n^{th} shell
T	temperature
u	radial displacement
α	thermal expansion coefficient (mean)
α_{inst}	instantaneous thermal expansion coefficient
$\alpha_{T_o,T}$	mean thermal expansion coefficient between temperature T_o and T
$\epsilon_{T_o,T}$	fractional expansion due to temperature increase from T_o to T
ν	Poisson's ratio
$\sigma_{r,t}$	stress, radial or tangential
Σ_n	defined as $\sum_{i=1}^{n} \frac{r_i^3 - r_{i-1}^3}{3} q_i$

10 REFERENCES

Binns, Ian M. (1964). - A comparison of thermo-elastic stress and temperature distribution in nuclear pebble bed reactor spheres with fully and partially dispersed fuel. AAEC/TM236.

Baltrukonis. (1959). - Comparison of approximate solutions of the thermo-elastic problem of the thick walled tube. J. of Aero/Space Science, Volume 26, No: 6. June, 1959.

Hawker, P. A. E., and Ridgway, N. W. (1965). - The expansion of a function in terms of Chebyshev polynomials using the IBM 7040. AAEC/TM293.

Morozov, E. M., and Fridman, Ya. B. (1961). - Thermal stresses and their calculation, contained in strength and deformation in non-uniform temperature fields, edited by Professor Ya. B. Fridman. Translated from the Russian and published by Consultants Bureau Enterprises Inc. New York, 1964.

Ralston, A., and Wilf, H. (1959). - Mathematical Methods for Digital Computers, John Wiley and Sons, London.

Timoshenko, S., and Goodier, J. N. (1951). - Theory of Elasticity. McGraw Hill Book Company. New York.

Turner, D. N., and Smith, P. D. (1965). - Linear thermal expansion of beryllia. AAEC/TM300.

Veevers, K., and Rotsey, W. B. (1966a). - The mechanical properties of dispersions of thoria in beryllia. AAEC/TM341, and Journal of Material Sciences, Volume 1, page 346.

Veevers, K., and Rotsey, W. B. (1966b). - The mechanical properties of BeO-(U,Th) O_2 dispersion fuels. AAEC/TM338.

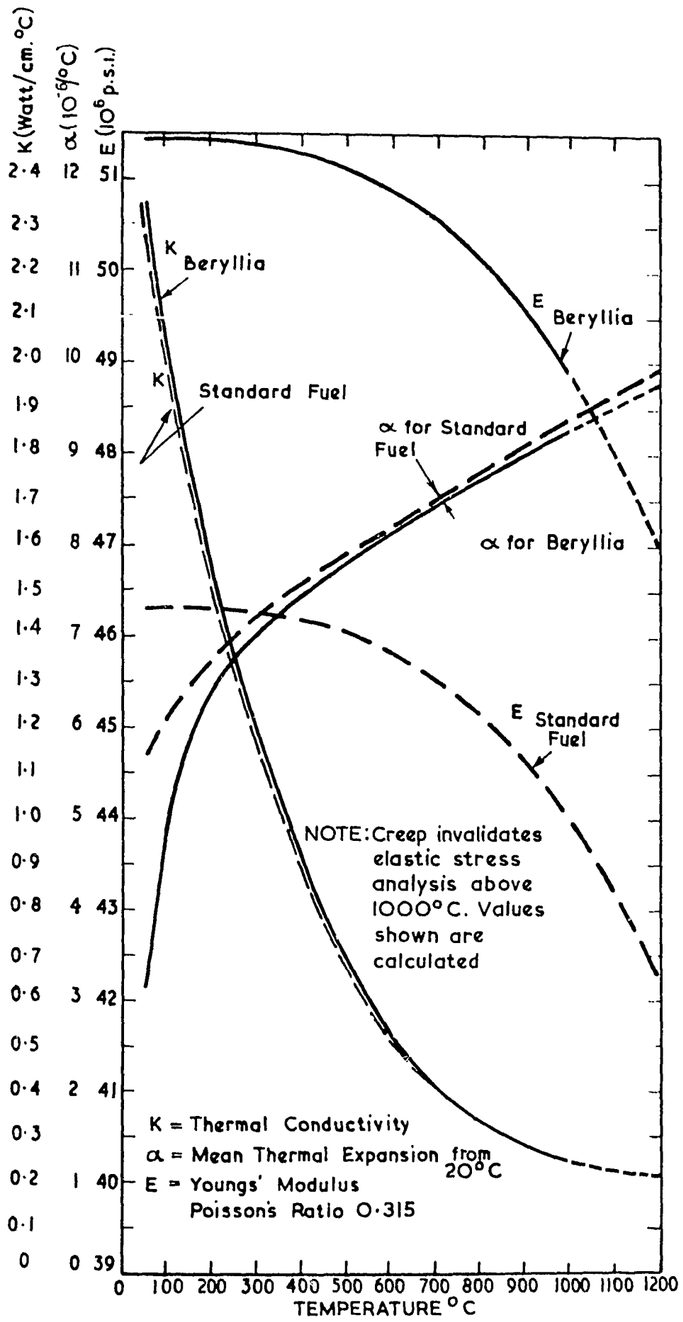

FIGURE 1. MATERIAL PROPERTIES USED FOR BERYLLIA AND STANDARD FUEL

P1081

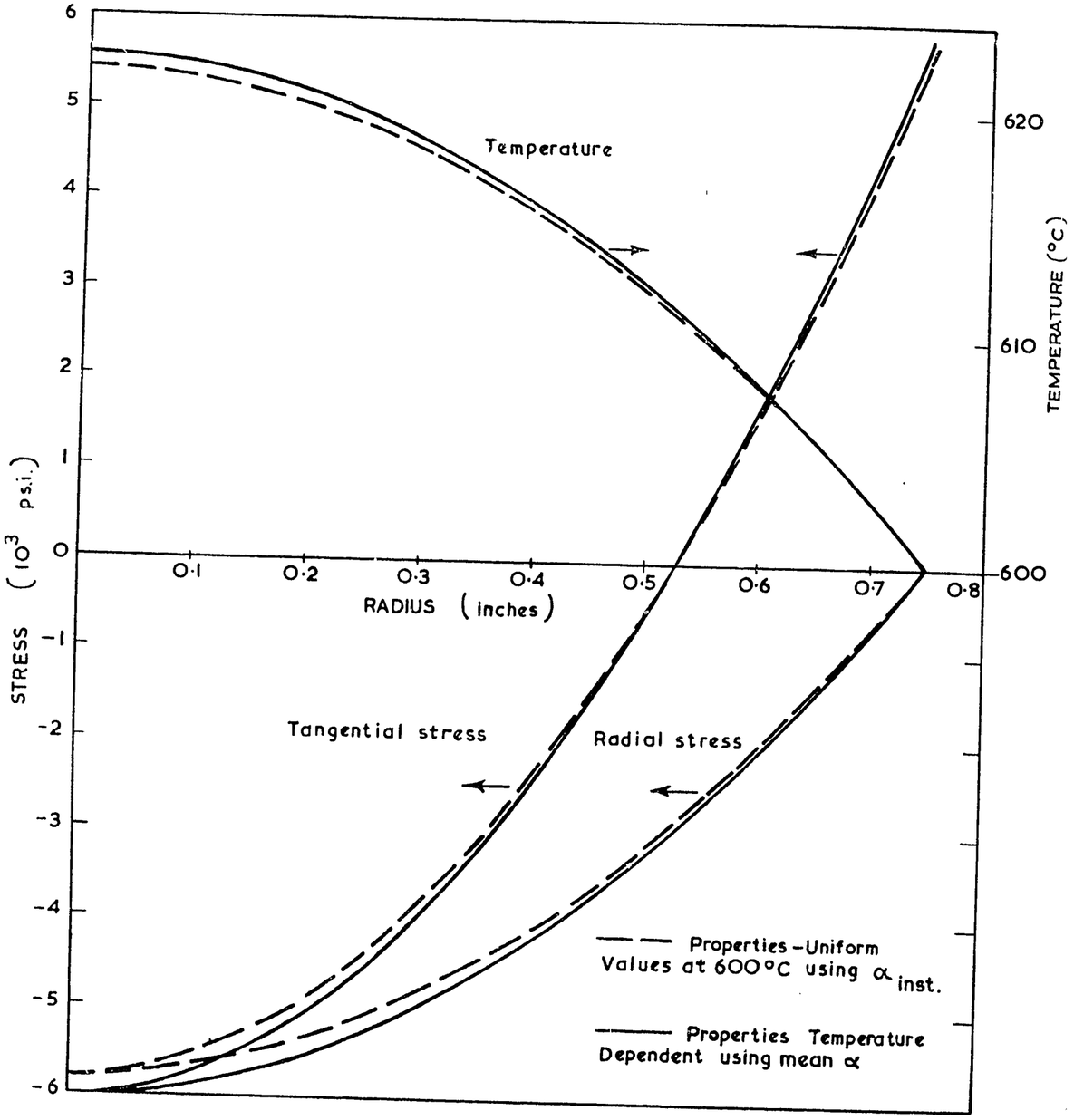

FIGURE 2. STRESS AND TEMPERATURE DISTRIBUTION IN SPHERICALLY SYMMETRIC UNCOATED FUEL ELEMENT (Standard Fuel, Unirradiated, Power Density 18.1818 Watts/cm³, Dia. 1.5 in., Surface Temperature 600°C)

P108f

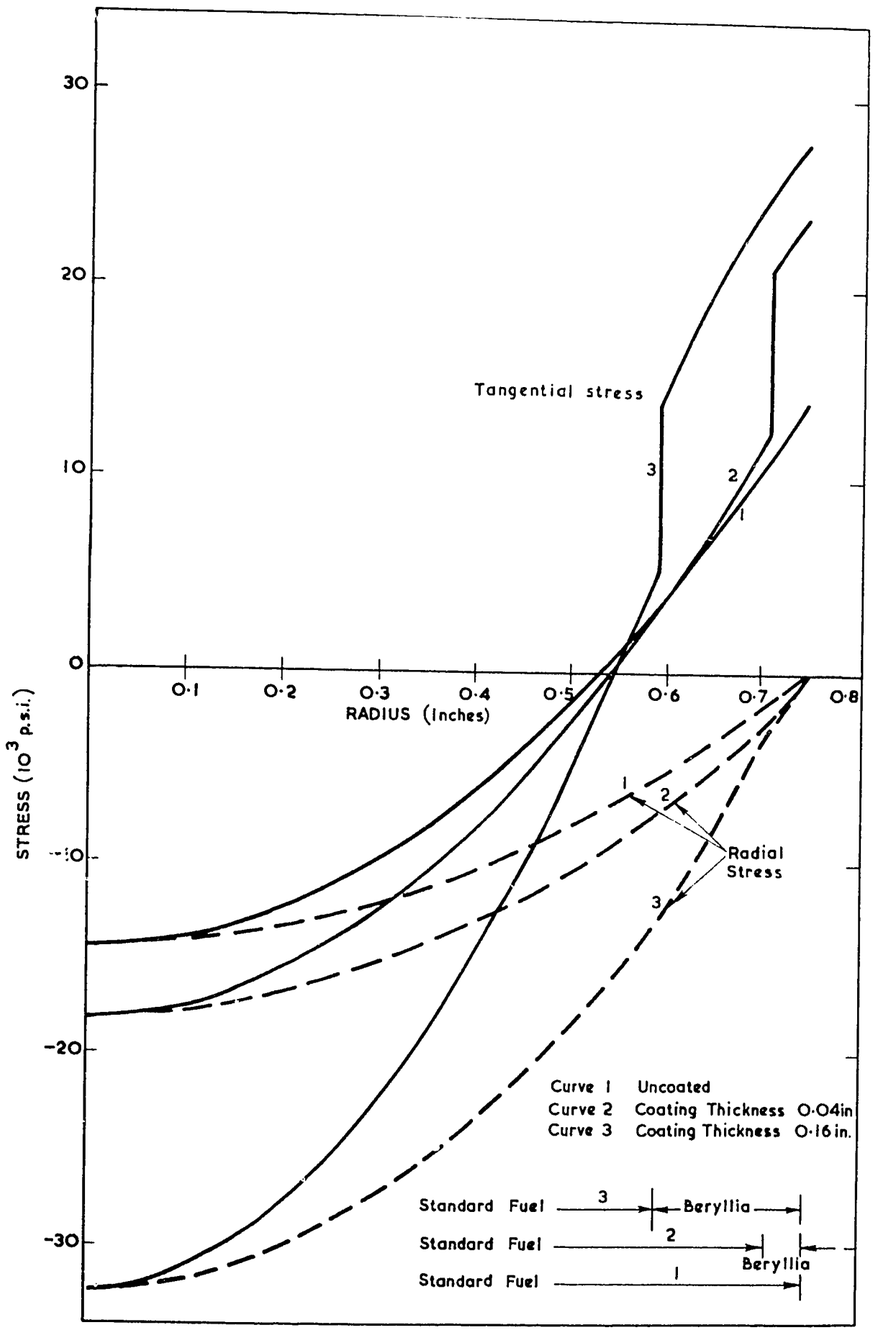

FIGURE 3. STRESS DISTRIBUTION IN SPHERICAL SYMMETRIC FUEL ELEMENTS OF STANDARD FUEL WITH BERYLLIA COATINGS (Surface Temperature 1000° C, Zero Stress at 20°C, Power Density, Mean 18.1818 Watts/cm³)

P108f

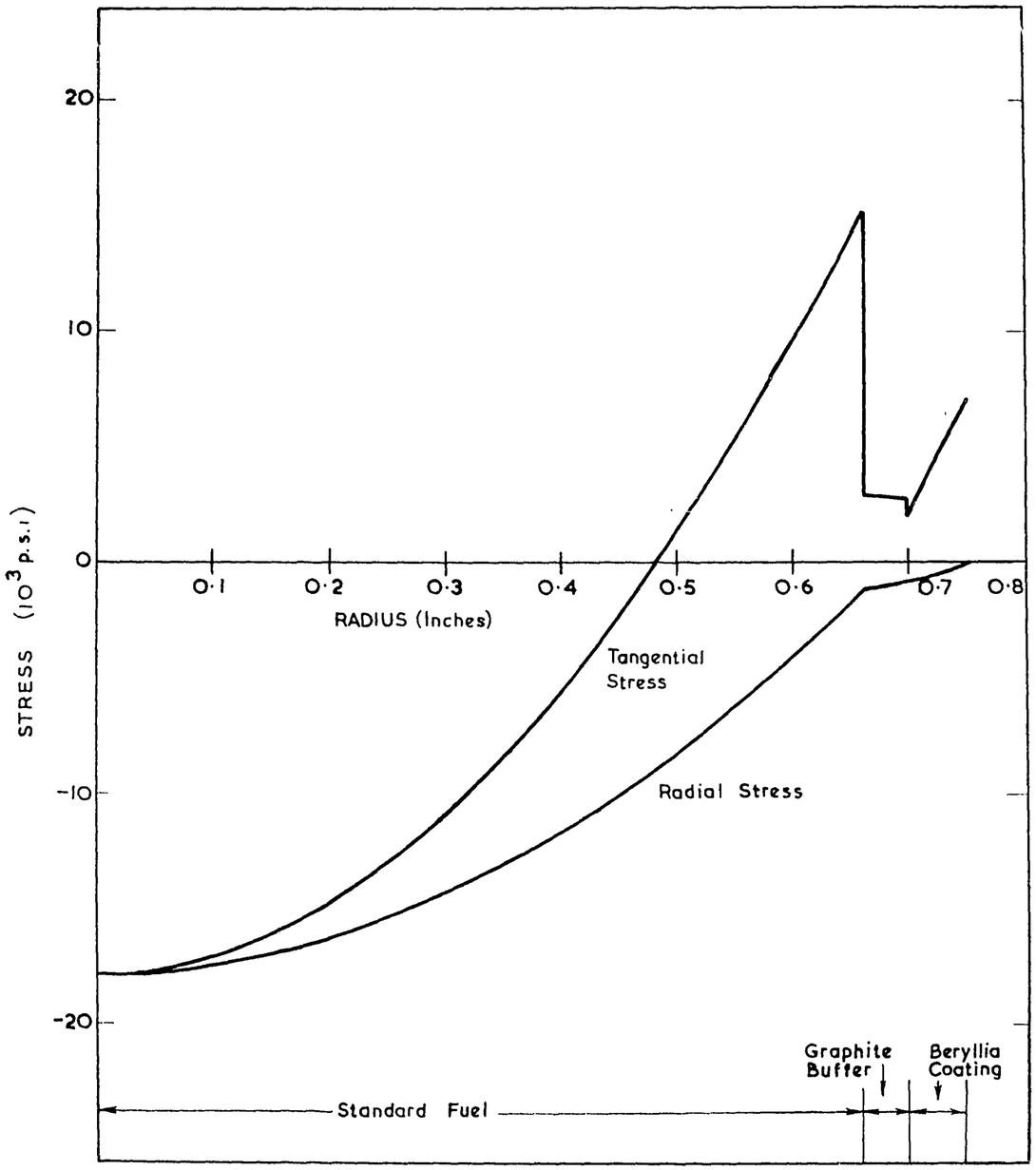

FIGURE 4. STRESS DISTRIBUTION IN SPHERICALLY SYMMETRIC FUEL ELEMENT WITH BERYLLIA COATING ON STANDARD FUEL CORE WITH GRAPHITE INTERLAYER (Power Density, Mean 18.1818 Watts/cm^3, Dia. 1.5 in., Surface Temperature 1000°C, Zero Stress at 20°C)

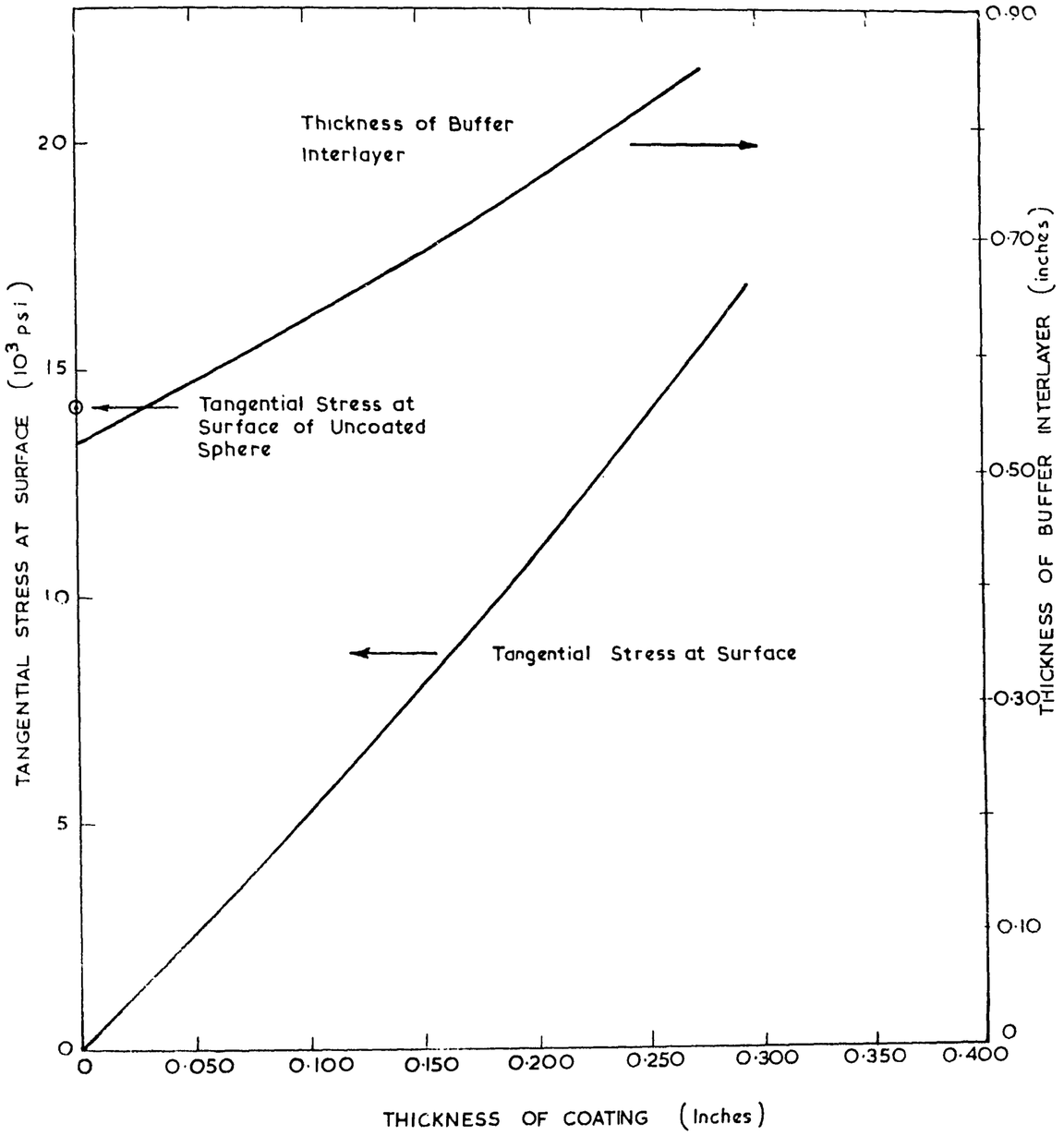

FIGURE 5. OPTIMUM GRAPHITE BUFFER INTERLAYER BETWEEN BERYLLIA COATING AND STANDARD FUEL CORE (Power Density, Mean 18.1818 Watts/cm^3, Dia. 1.5 in., Surface Temperature 1,000°C, Zero Stress at 20°C)

P1081

P1081

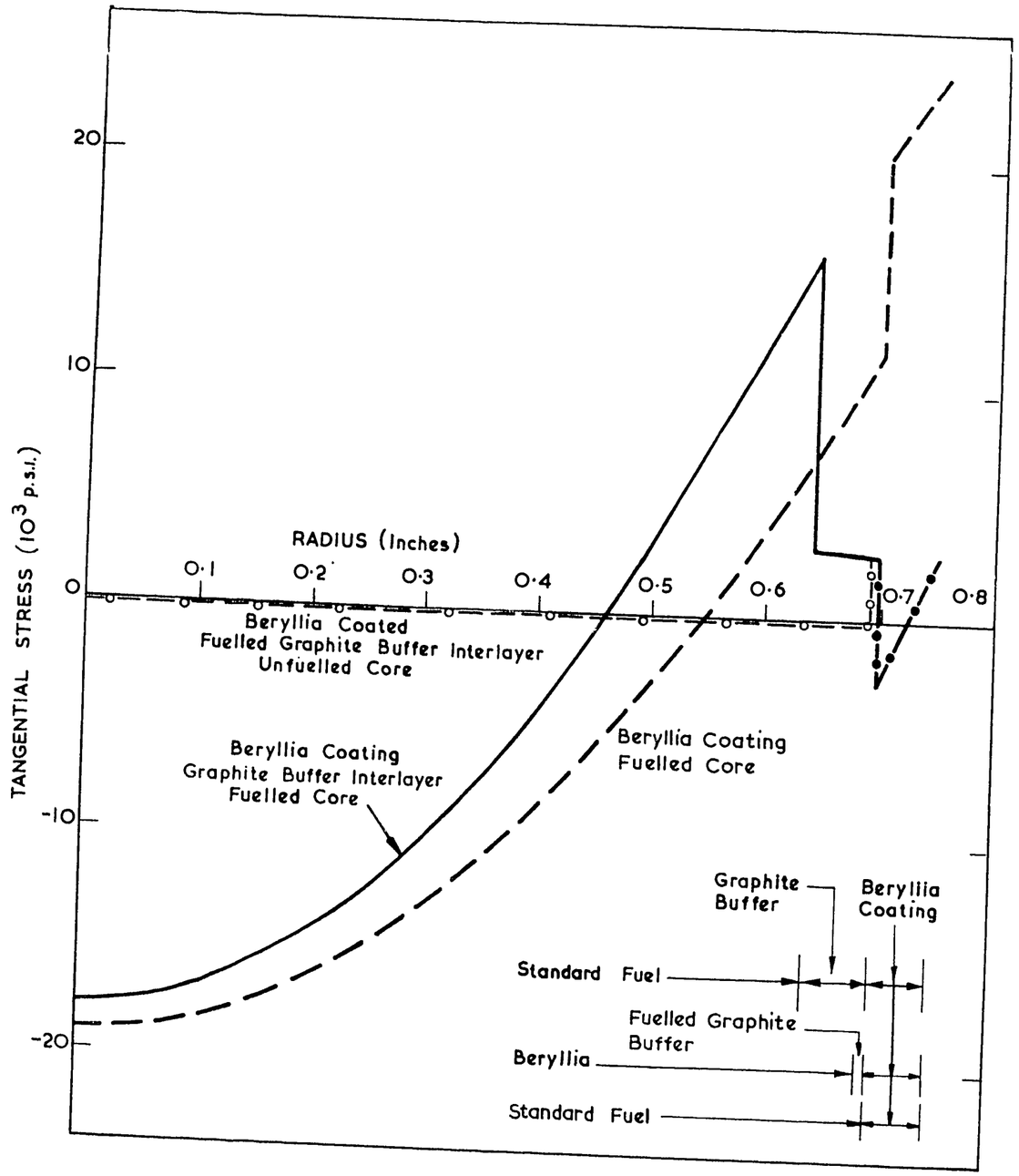

FIGURE 6 TANGENTIAL STRESS DISTRIBUTION IN FUEL ELEMENTS WITH BERYLLIA COATING (0.050 in. Thick, Surface Temperature 1000°C, Zero Stress at 20°C)

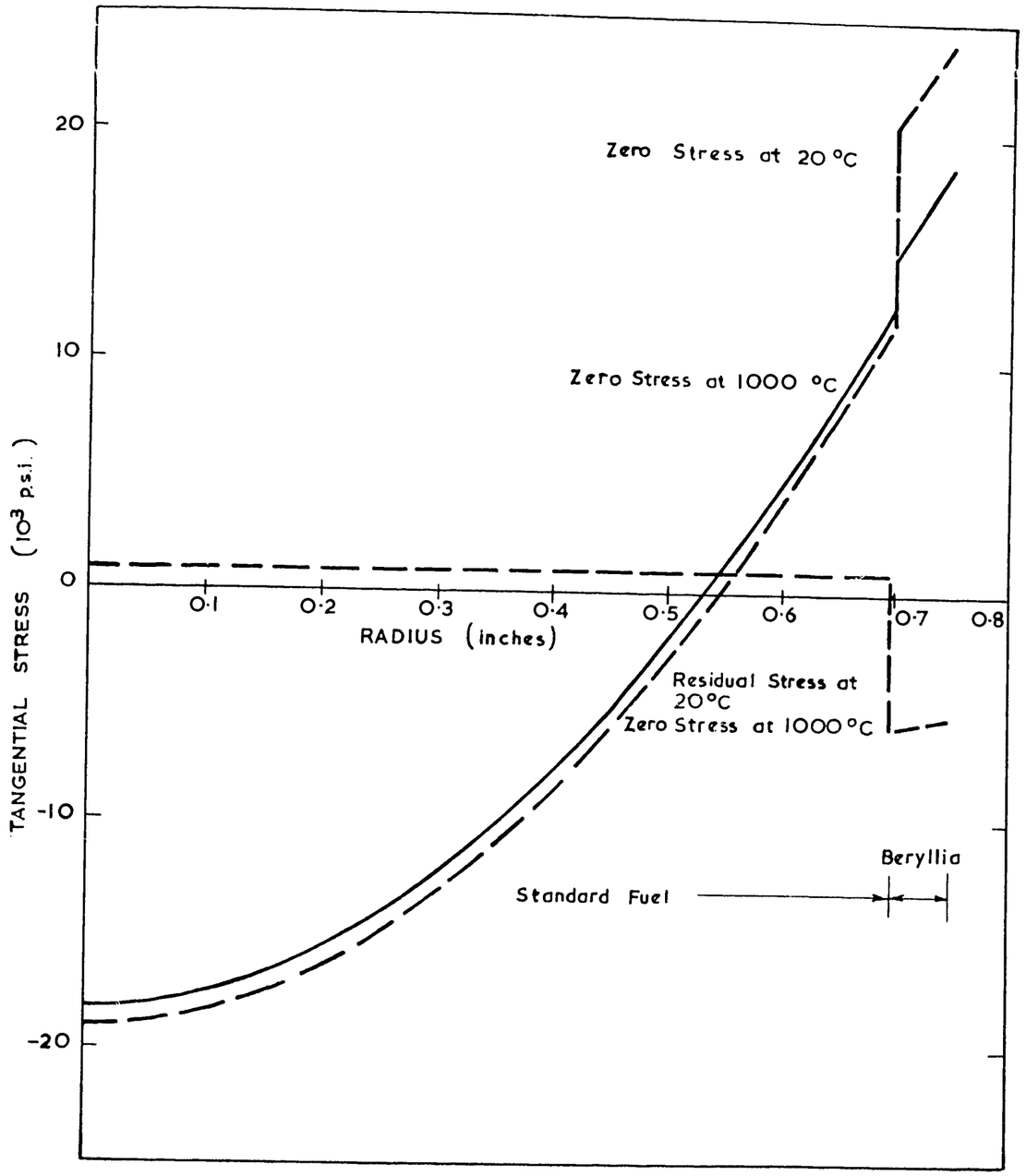

FIGURE 7. TANGENTIAL STRESS DISTRIBUTION IN FUEL ELEMENT SHOWING RESIDUAL STRESS (Beryllia Coating on Standard Fuel, Power Density 18.1818 Watts/cm^3, Dia. 1.5 in., Surface Temperature 1000°C)

P1081

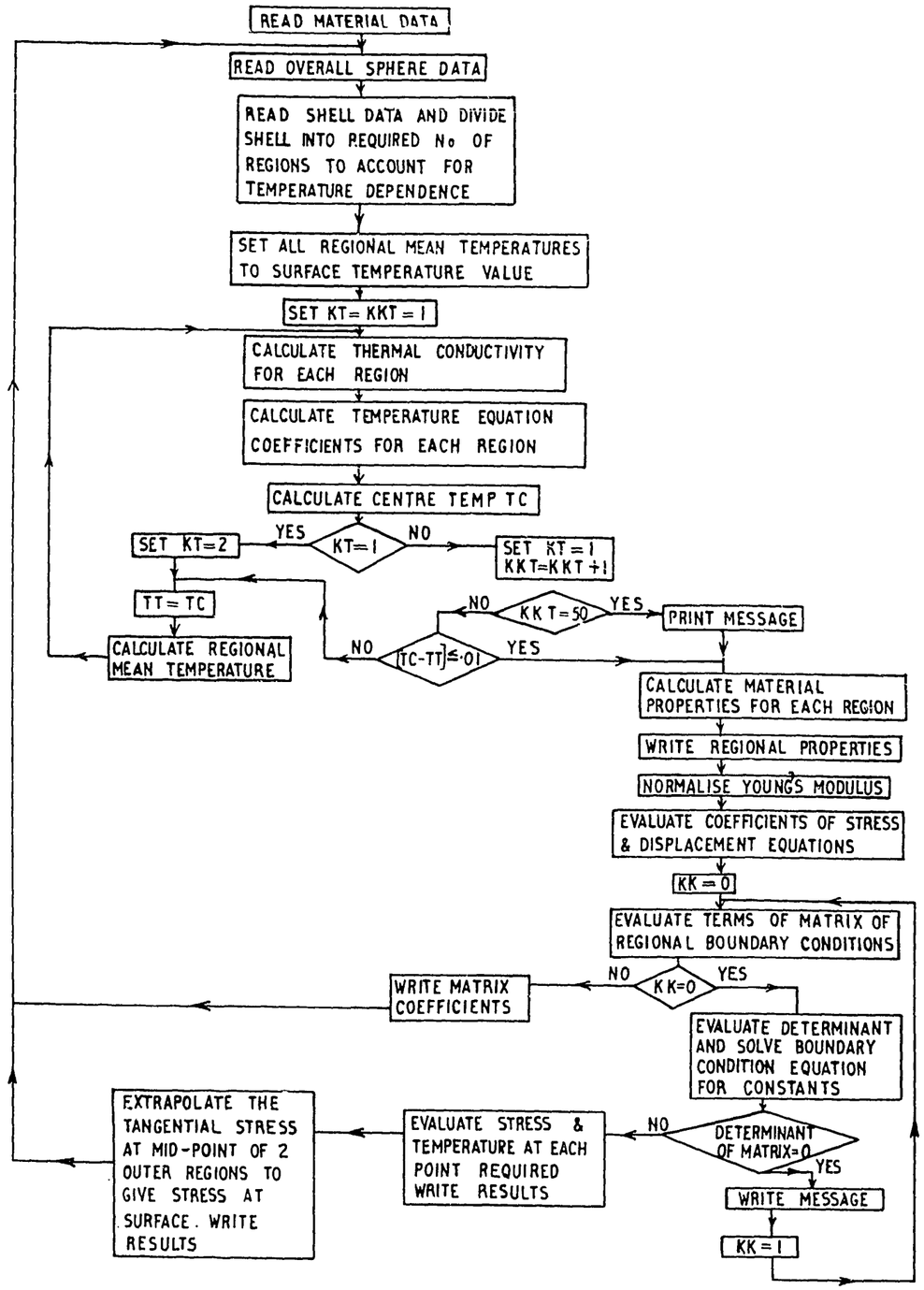

FIGURE 8. 'MULTI' COMPUTER PROGRAMME FLOW CHART

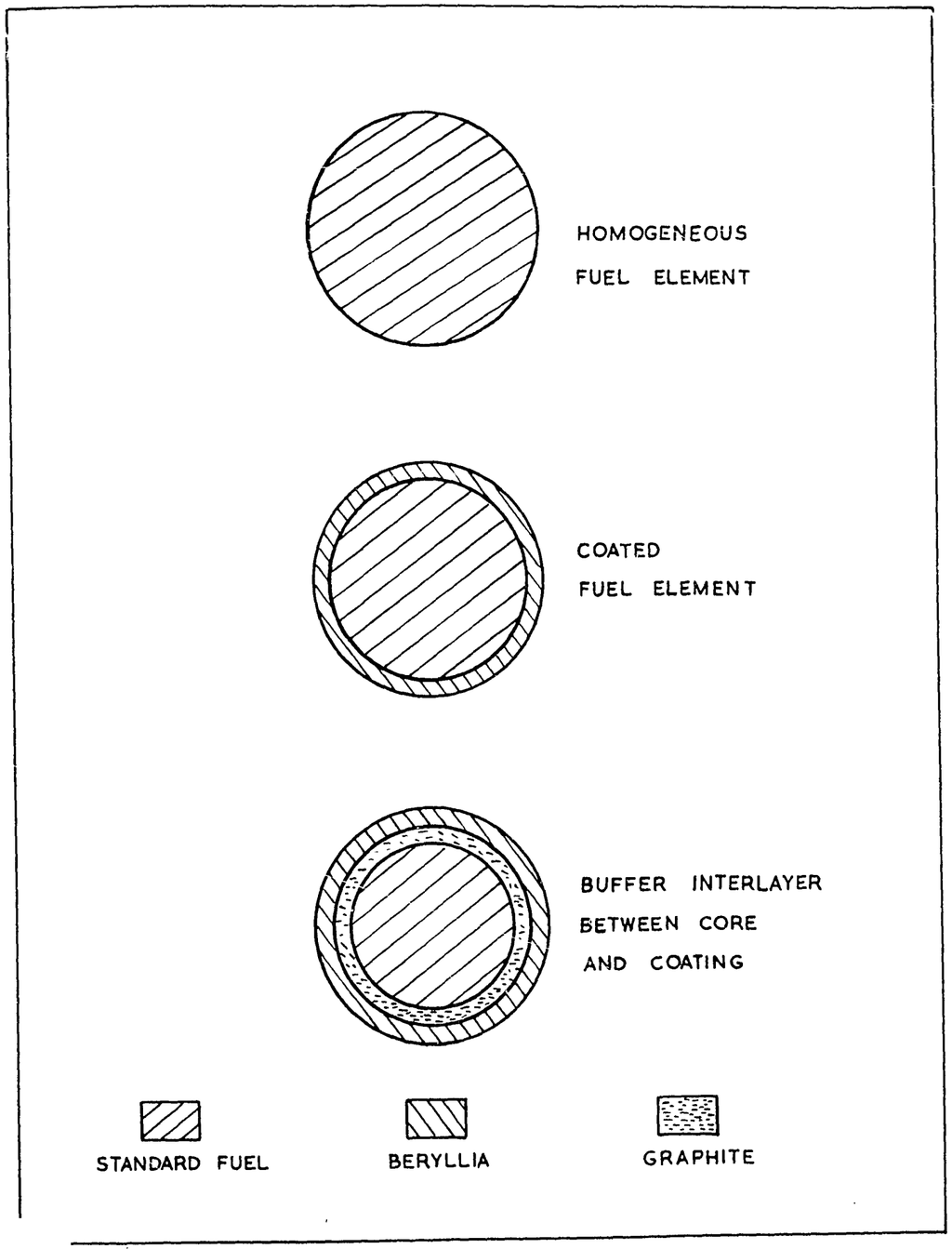

FIGURE 9. FUEL ELEMENT CONFIGURATIONS